

# Performance of Very Low Dark Current SWIR PIN Arrays

Joseph Boisvert<sup>\*</sup>, Takahiro Isshiki, Rengarajan Sudharsanan, Ping Yuan,  
and Paul McDonald

Spectrolab Inc., a Boeing Company, 12500 Gladstone Ave., Sylmar, CA, USA 91342

## ABSTRACT

Boeing Spectrolab has grown, fabricated and tested InGaAs PIN arrays with less than 1 nA/cm<sup>2</sup> dark current density at 280 °K. The PIN diodes display greater than 1 A/W responsivity at -100 mV reverse bias with about 50 fF of diode capacitance.

## 1. INTRODUCTION

In photon counting imaging applications a focal plane array consisting of a detector and readout integrated circuit (ROIC) array must both be low noise. At room temperature, InGaAs PIN detector arrays are most suitable because the required signal bandwidth is fairly modest and the first stage input amplifiers on the ROIC can be very low noise. However, in many applications relatively long integration times demand that the input dark current from the PIN detector be held to an absolute minimum to retain photon counting sensitivity. In some cases this means that the dark current specification flowed down to the PIN pixel calls for less than 10 fA of dark current. This is a very demanding specification that requires both very high quality material as well as careful attention to device design and processing.

Under the funding from Raytheon from the DARPA Photon Counting Array (PCAR) program, Spectrolab has been developing very low noise InGaAs PIN arrays for SWIR imaging applications. 1280x1024 arrays have been fabricated and test structures evaluated for performance. These results to date indicate that high quantum efficiency and low dark current PINs have been developed to meet the PCAR Phase II requirements.

## 2. MATERIALS AND DEVICE DESIGN AND CHARACTERIZATION

Figure 1 displays a cross section of the epitaxial layer stack that forms the planar PIN diode. The device layers were grown by metal-organic vapor phase epitaxy (MOVPE) on 2" sulphur-doped (100) InP. Trimethylindium, trimethylgallium, 100% arsine, and 100% phosphine were used as source materials. Dimethyl zinc was used as a source dopant for patterned diffusion into the InP cap layer.<sup>1</sup> 1280x1024 element PIN arrays were fabricated using a test mask that also includes several diagnostic structures: guarded 40 μm diameter single element diodes, guarded 10x10 μm<sup>2</sup> commoned arrays with various diffusion areas ranging from 10x10 μm<sup>2</sup> to 24x24 μm<sup>2</sup>. The test mask pattern is shown in Figure 2.

Materials characterizations conducted on calibration layers prior to the complete device epitaxial growth included x-ray diffraction, photoluminescence, electrochemical capacitance-voltage profiles, and Hall effect mobility characterizations. Figure 3 displays the Hall effect mobility characterization of unintentionally-doped Spectrolab InP material. The high electron mobility correlates very well with published data and indicates very high quality material.<sup>2</sup>

Post fabrication measurements include current-bias characterization with and without 1550 nm illumination, dark current-bias characteristics at several temperatures, and collection of capacitance-voltage characteristics at room temperature.

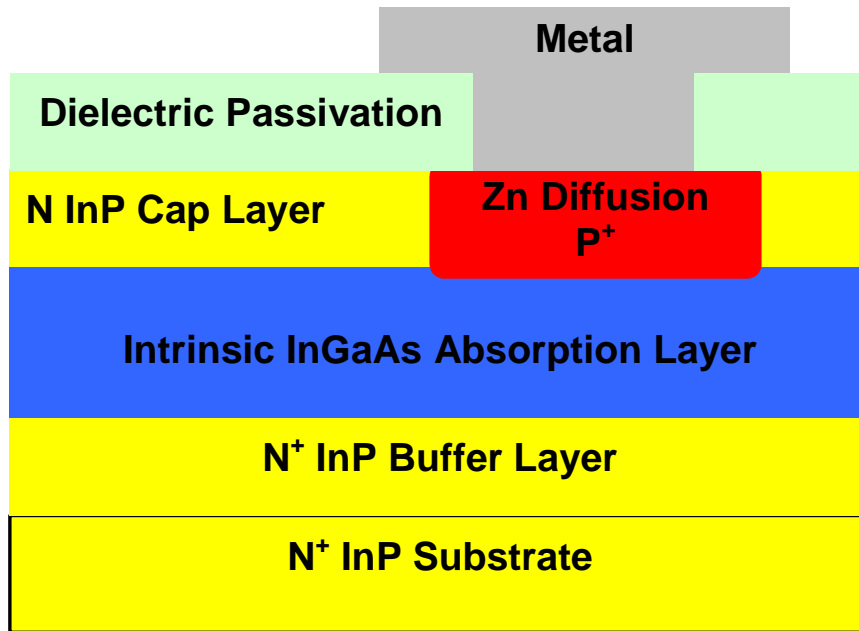


Figure 1. A cross section of the InGaAs/InP PIN.

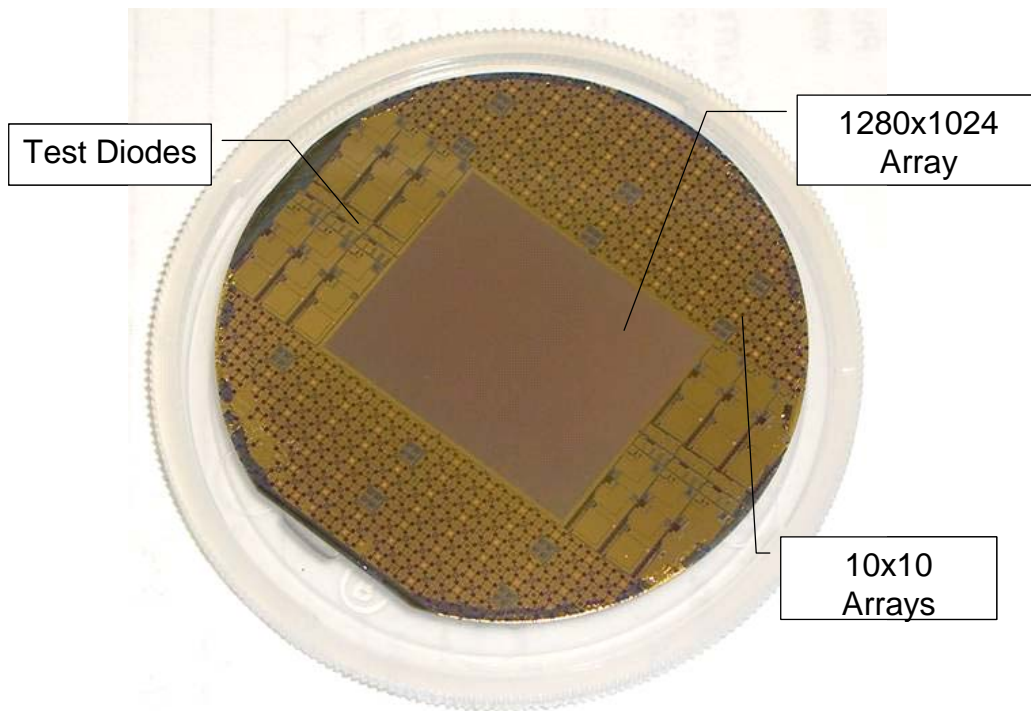


Figure 2. A photograph of a processed 2" InGaAs/InP PIN wafer

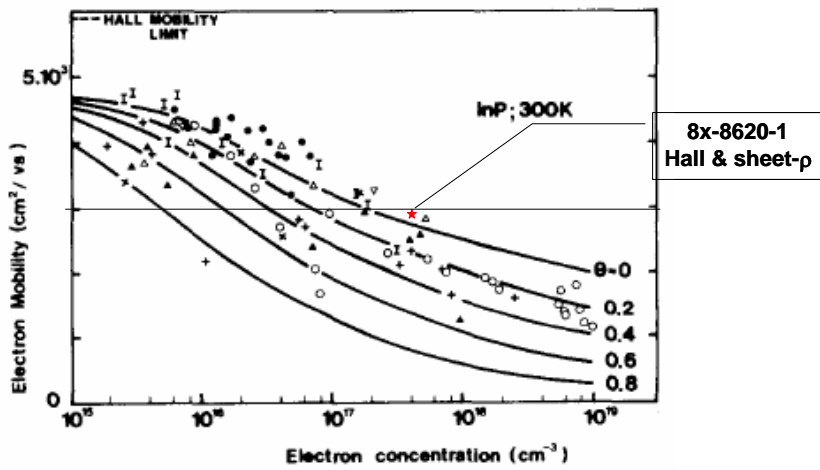


Figure 3. The electron mobility of unintentionally-doped InP.

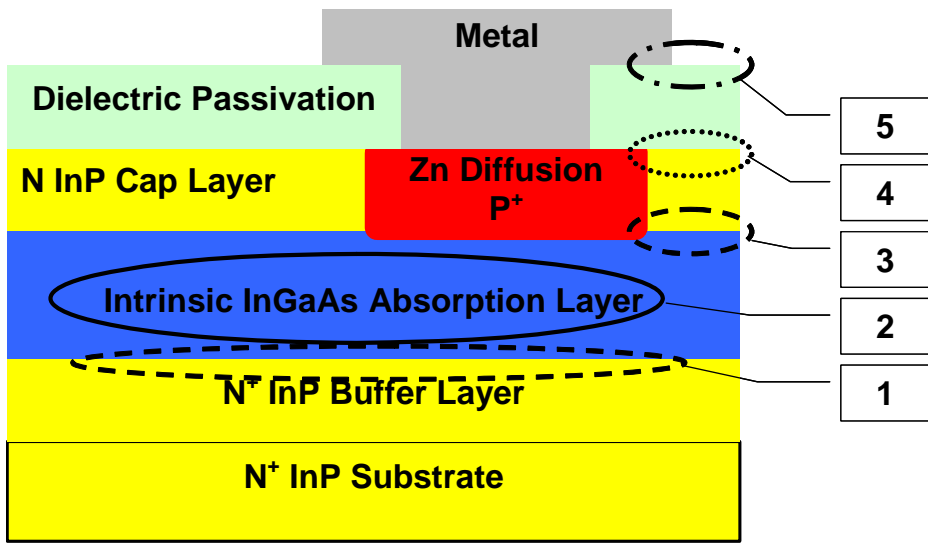


Figure 4. There are several locations within a planar PIN diode that can contribute to dark current. (1) the interface between the buffer and absorber layers. (2) the quality of the absorber layer bulk material. (3) the interface between the absorber and cap layers. (4) the interface between the cap layer and dielectric passivation. (5) the top of the dielectric passivation layer.

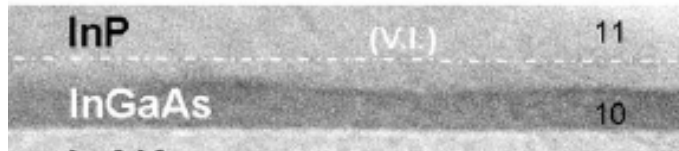


Figure 5. The interface between InGaAs and InP is well known to be non-stoichiometric due to phosphorus replacement of arsenic in the InGaAs layer during growth.

#### 4. RESULTS AND DISCUSSION

Under the PCAR program several areas for dark current reduction have been identified and are illustrated in Figure 4. In particular the interface between the InGaAs absorber and InP cap layer is well known to present a non-stoichiometric region due to phosphorus kick-out of arsenic in GaAs bonds.<sup>3,4</sup> A perimeter-to-area (P/A) study was carried out in the first phase of the PCAR program that identified this particular interface as a source of dark current that would be especially troublesome for small area pixels (on the order of 15-20  $\mu\text{m}$  square) operating at 280 °K where perimeter generation current can dominate. Figure 6 shows a typical 280 °K P/A analysis indicating that the diodes are perimeter current dominated. Equation 1 indicates how the dark current data at a given bias for several diodes is reduced. The slope of the characteristic in Figure 6 is proportional to the diode perimeter generation current. In this case the intercept was negative as fit and indicates that the bulk current density was so small as to be within measurement error and not resolvable using this technique.

Large area diodes with very small P/A ratios were used to accurately determine the bulk current density. The data shown in Figure 7 indicate that the that bulk dark current at 283 °K was sufficiently small to meet the Phase I PCAR goal of  $<2 \text{ nA/cm}^2$ . However the perimeter current would dominate and small pixel diodes would not meet the Phase I goal.

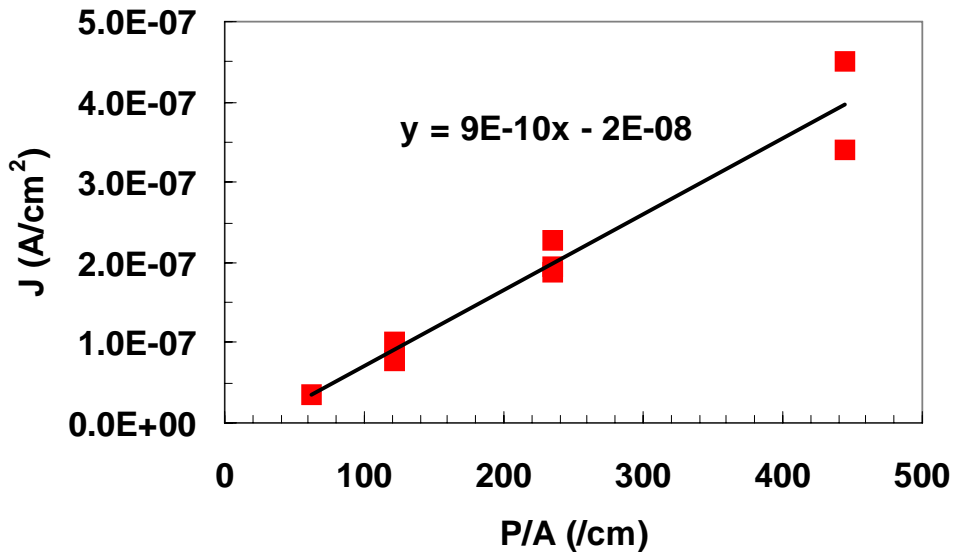


Figure 6. The dark current density versus P/A ratio is used to characterize the bulk and surface component contributions to the measured dark current at -100 mV reverse bias and 280 °K. The intercept of the characteristic is the bulk dark current density; the slope yields the perimeter dark current. Note that in this case the bulk dark current density is not well determined as the intercept is so small as to fall within measurement error.

$$I = I_B A + I_S P$$

$$J = \frac{I}{A} = I_B + I_S \frac{P}{A}$$

Equation 1. The bulk and perimeter dark current components are identified through this model that breaks out the bulk and perimeter dark current contributions. Variable perimeter-to-area, constant perimeter (variable area) and constant area (variable perimeter) test diodes shown in Figure 2 were characterized and those data reduced and shown in Figure 6.

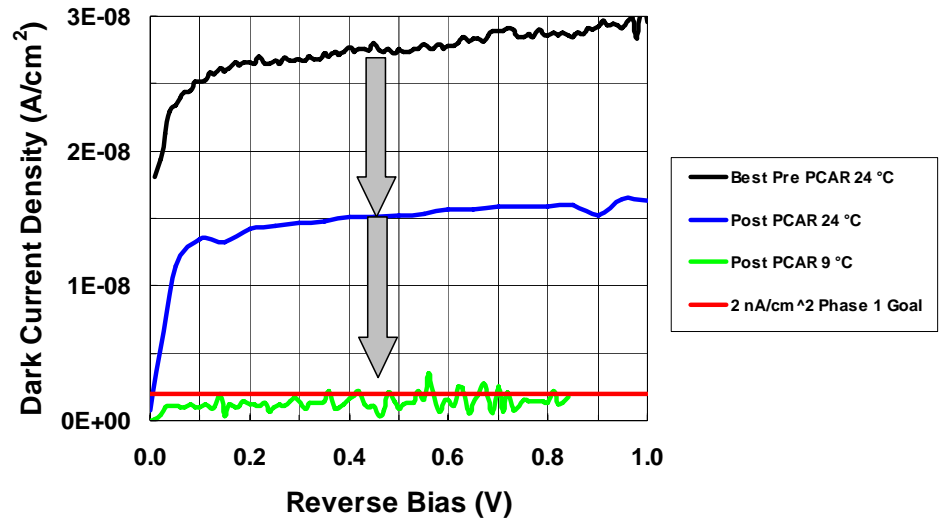


Figure 7.

The dark current density versus reverse bias for large area ( $> 7 \times 10^4 \mu\text{m}^2$ ) PIN diodes. The top curve is the best performance prior to the PCAR program ( $\sim 25 \text{ nA/cm}^2$ ) at room temperature and 100 mV reverse bias. The middle curve shows the PCAR post Phase I data ( $\sim 13.5 \text{ nA/cm}^2$ ) at room temperature and 100 mV reverse bias). The bottom characteristic is taken at 282 °K and is about  $1 \text{ nA/cm}^2$ .

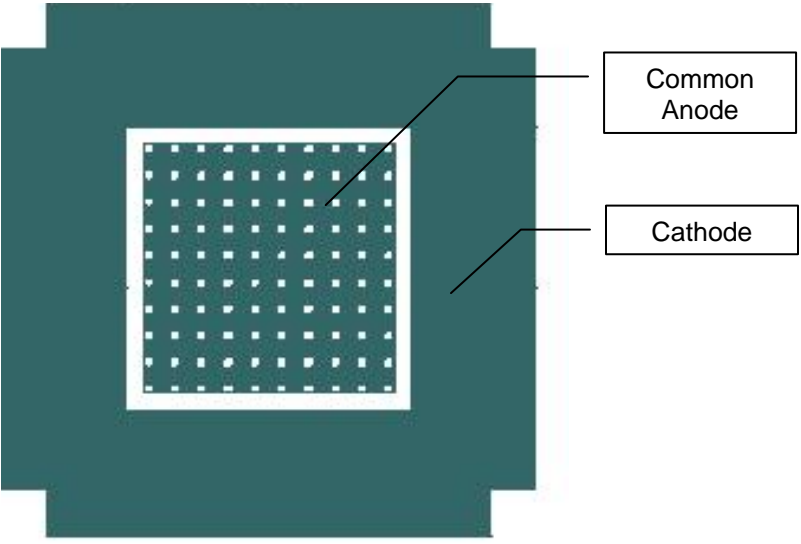


Figure 8.

The mask layout for a common anode 10x10 element PIN array.

After modifications to the epitaxial structure, dark I-V data were collected on 10x10 element arrays like those shown in Figure 8. In this configuration all 100 pixels are put in parallel by a blanket metallization as shown in the figure. The resulting current bias characteristic for one of those arrays collected at room temperature is shown in Figure 9. The room temperature dark current density of 15.6 nA/cm<sup>2</sup> at -100 mV reverse bias for the small pixel array is about the same as for the large diodes shown in Figure 8. The dark current density versus temperature as measured at -100 mV reverse bias is shown in Figure 10. This Arrhenius plot shows that the dark current density is dominated by diffusion current down to about 283 °K. The dark current density drops below 2 nA/cm<sup>2</sup> at about 279 °K.

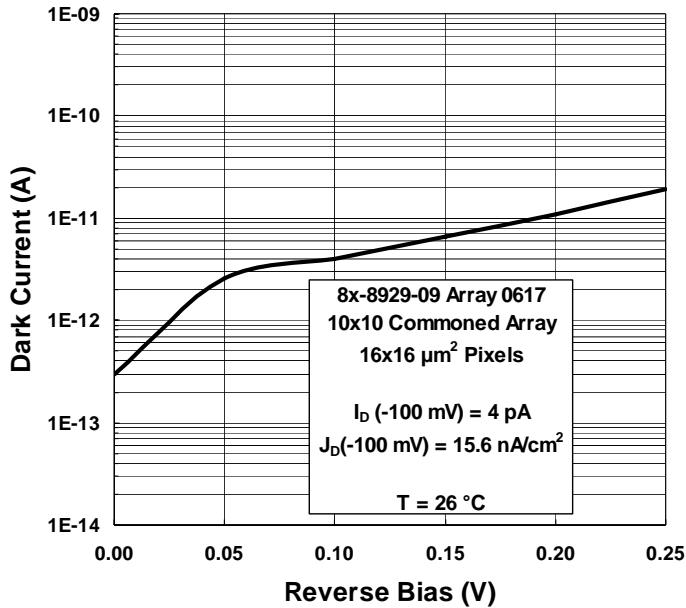


Figure 9. The dark current versus reverse bias characteristic for a 100 element array with all the pixels in parallel.

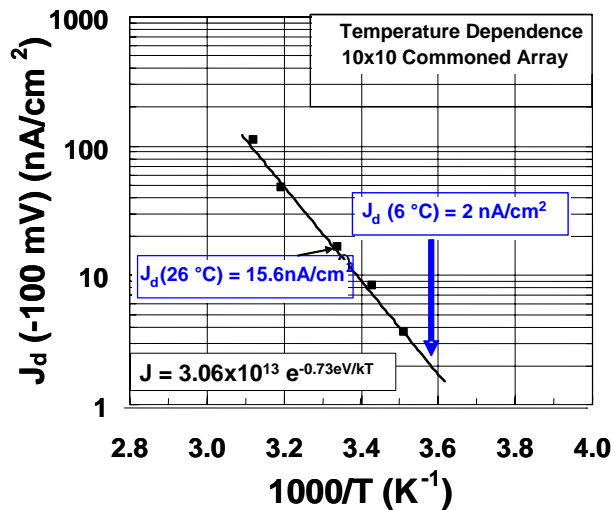


Figure 10. The dark current density at -100 mV reverse bias at several different temperatures for a 100 element commoned array. The Arrhenius plot shows a thermal activation energy of 0.73 eV. This activation energy is consistent with a diffusion limited current density.

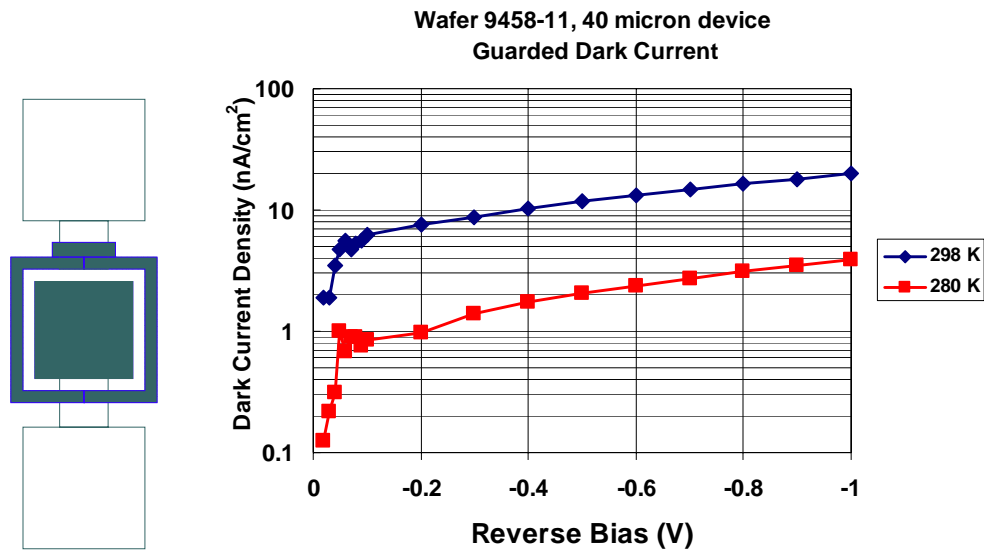


Figure 11. A 40  $\mu\text{m}$  square guarded test structure and the measured dark I-V characteristics.

In Phase II of the PCAR program the effort to reduce dark current density has continued. Additional modifications to the epitaxial structure shown in Figure 1 have resulted in further improvements. The data shown in Figure 11 are collected on a test structure where a guard ring has been diffused around the active  $40 \times 40 \mu\text{m}^2$  diode. During the dark current versus bias measurement the outer guard ring is kept at the same bias as the diode anode contact, thus eliminating any potential gradient to outside ground points. This configuration is representative of array operation where all interior array pixels will be surrounded by nearest neighbors that are held at the same potential through their read out amplifiers. In this configuration the dark current density at 298 °K is about  $5 \text{ nA/cm}^2$ ; at 280 °K the dark current density falls to about  $0.7 \text{ nA/cm}^2$ .

As confirmation of this low dark current performance, several 100 element arrays were measured in a guarded condition at 280 °K and those data are detailed in Table 1. The dark current densities on these 7 arrays average about  $0.72 \text{ nA/cm}^2$ , consistent with data collected on the  $40 \mu\text{m}$  square test structure of Figure 11.

ID	Area ID	$J_d$ nA/cm <sup>2</sup>
14-11	D10	0.66
13-11	D10	0.68
16-11	D10	0.69
15-11	D10	0.72
16-23	D10	0.75
15-09	D12	0.75
16-09	D12	0.78

Table 1. The pixel dark current density measured at 280 °K under a reverse bias of -100 mV. Guarded  $10 \times 10$  common anode arrays were used to make these measurements. These data are consistent with those measured on the  $40 \mu\text{m}$  square guarded test structure shown in Figure 11.

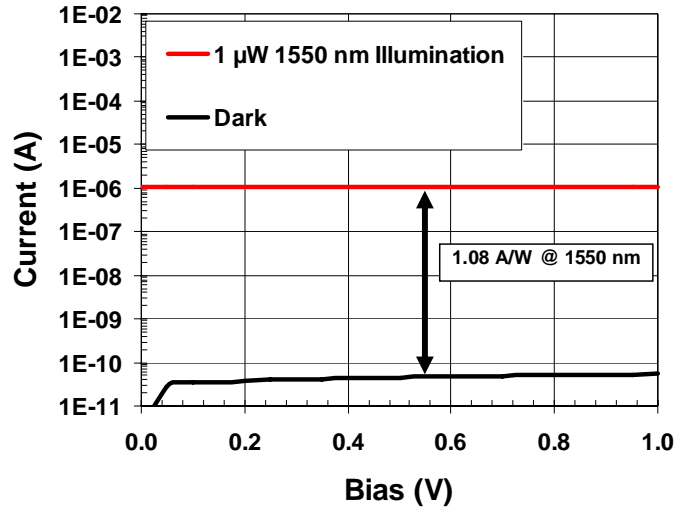


Figure 12. The measured optical response of a planar, front-illuminated InGaAs/InP PIN diode. The measured responsivity is 1.08 A/W at 1550 nm. The optical response on a reverse-illuminated array pixel is expected to be higher due to a reflection at the indium bump metallization.

While dark current density is an important figure-of-merit for imaging PIN arrays, optical responsivity is also of obvious importance. Figure 12 shows the measured optical response of a front-illuminated planar PIN diode test structure. The responsivity at 1550 nm is about 1.1 A/W; the responsivity for a reverse-illuminated pixel is expected to be greater than 1.1 A/W because of an extended optical path length from indium bump metallization.

Pixel capacitance is also of importance because it impacts the input-referred amplifier noise. Figure 13 displays the capacitance versus diode area characteristic measured on several different planar PIN diode test structures. The capacitance is measured at -100 mV reverse bias. The data indicate that for a 15 μm pitch array (the PCAR Phase II format) that a pixel with about an 8 μm diffused area will have about 50 fF input capacitance.

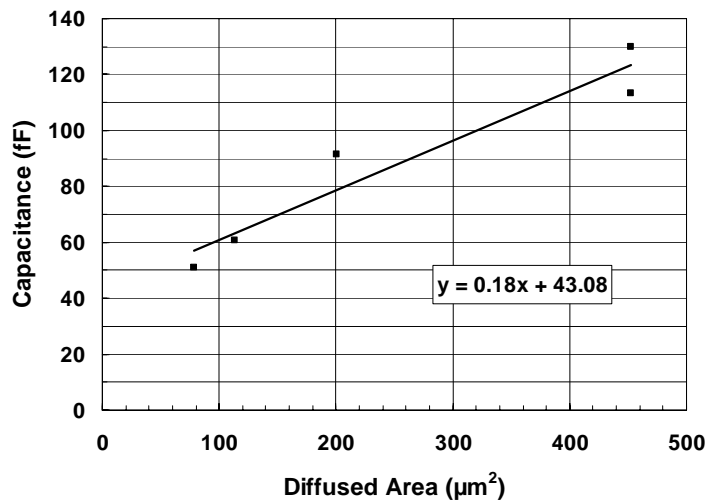


Figure 13. The measured room temperature versus area diode capacitance at -100 mV reverse bias. These data were collected on several different test diode structures.

## 5. SUMMARY

Spectrolab has developed extremely high quality InGaAs/InP imaging PIN diode arrays for SWIR applications. In two phases of the DARPA PCAR program the dark current density at 280 °K has dropped to about 0.7 nA/cm<sup>2</sup> while still maintaining excellent optical responsivity of greater than 1 A/W. These results have been achieved through continuous improvement in material quality and device design.

Acknowledgement: The low dark current InGaAs work was funded by Raytheon as part of the DARPA PCAR program.

## REFERENCES

1. A. van Geelen, T.M.F. de Smet, T. van Dongen, W.M.E.M. van Gils "Zinc doping of InP by metal organic vapour phase diffusion (MOVPE)" J. Crystal Growth 195, 79 (1998).
2. W. Walukiewicz, J. Lagowski, L. Jastrzebski, P. Rave, M. Lichtendteiger, C.H. Gatos, and H.C. Gatos "Electron mobility and free-carrier absorption in InP; determination of the compensation ratio" J. Appl. Phys. 51, 2659 (1980).
3. J. Decobert, G. Patriarche "Transmission electron microscopy study of the InP/InGaAs and InGaAs/InP heterointerfaces grown by metalorganic vapor-phase epitaxy" J. Appl. Phys. 92, 5749 (2002).
4. J. Boisvert, T. Isshiki, R. Sudharsanan, P. Yuan, and P. McDonald, "Design of very low dark current SWIR PIN arrays" 2006 Digest of the 17-19 July LEOS Summer Topical Meetings, 54 (2006).

[\\*jboisvert@spectrolab.com](mailto:*jboisvert@spectrolab.com); phone 1 818 838 2610; fax 1 818 838 7474; [www.spectrolab.com](http://www.spectrolab.com)